Article published online: 2023-12-13

Durability of Photosensitizers in a Photo-oxidation Reaction in a Novel Oscillatory Baffled Photo Reactor

Jianhan Chen[1] Rohen Prinsloo[1] Xiongwei Ni[1]*

[1] Centre for Oscillatory Baffled Reactor Advancement, School of Engineering and Physical Sciences, Heriot–Watt University, Edinburgh, United Kingdom

Address for correspondence Xiongwei Ni, PhD, School of Engineering and Physical Sciences, Heriot–Watt University, Edinburgh EH14 4AS, United Kingdom (e-mail: x.ni@hw.ac.uk).

Pharmaceut Fronts 2023;5:e274–e281.

Abstract

With the rapid development of novel photosensitizers/photocatalysts, photochemical transformation has become possible and practical. In this context, we report for the first time our work on testing and quantifying the durability and robustness of a heterogeneous photosensitizer, polymer-supported rose Bengal (Ps-RB) beads, in a model photo-oxidation reaction between α-terpinene and singlet oxygen ($^1O_2$). A novel photo reactor is used due to its capabilities of providing uniform suspensions of solid beads and uniform light distribution. We have proposed a methodology for quantifying the durability of the beads including the factors of loss of beads and the reduced product concentration. The results show that the durability of the Ps-RB beads has decreased by about 67% after five consecutive runs, and the half-life of the beads can be reached in less than 200 minutes. In addition, we have also identified the optimal bead mass in the novel photo reactor. Our work not only enriches the designs of new and better photosensitizers but also provides a comprehensive methodology for testing and validating photosensitizers.

Keywords

- polymer-supported rose Bengal beads
- durability
- α-terpinene
- oscillatory baffled photo reactor
- ascaridole
- singlet oxygen

Introduction

The significantly increased interest in research and development of photochemistry has been driven by the fact that visible light is harnessed to initiate reactions and catalysis; novel photocatalysts/photosensitizers are rapidly being developed. This has promoted process innovations of synthesizing chemicals and pharmaceutical intermediates from unimolecular or radical chain reactions[1–7] to dual catalytic, bi- and multi-molecular transformations.[8–15] Photosensitizer/photocatalyst plays a critical role in this synthesis, so much so, that the advancement of heterogeneous photocatalysis (HPCat) has been described as one of the greatest challenges and opportunities within photochemistry.[16] One question that remains to be answered is how durable a photosensitizer/photocatalyst can be, which is the focus of this article. In this work, an HPCat photosensitizer, polymer-supported rose Bengal (Ps-RB) beads, is tested for its durability in a model photo-oxidation reaction between α-terpinene and singlet oxygen ($^1O_2$). A novel batch oscillatory baffled photo reactor (OBPR) is used because of its excellent capabilities of suspending solids and enabling uniform light distribution.

Reaction Scheme and Experimental Setup

Reaction Scheme

The photo-oxidation reaction is the well-known Diels–Alder-type reaction as shown in ►**Fig. 1** with Ps-RB porous beads as the heterogeneous photosensitizer. Photo absorption ($+h\nu$) by the Ps-RB chromophore under light irradiation is the first step of the reaction, which promotes an electron to a higher order singlet electronic excited state (^{1}[Ps-RB]*). The next

received
September 18, 2023
accepted
November 2, 2023
article published online
December 13, 2023

DOI https://doi.org/10.1055/s-0043-1777299.
ISSN 2628-5088.

Georg Thieme Verlag KG, Rüdigerstraße 14, 70469 Stuttgart, Germany

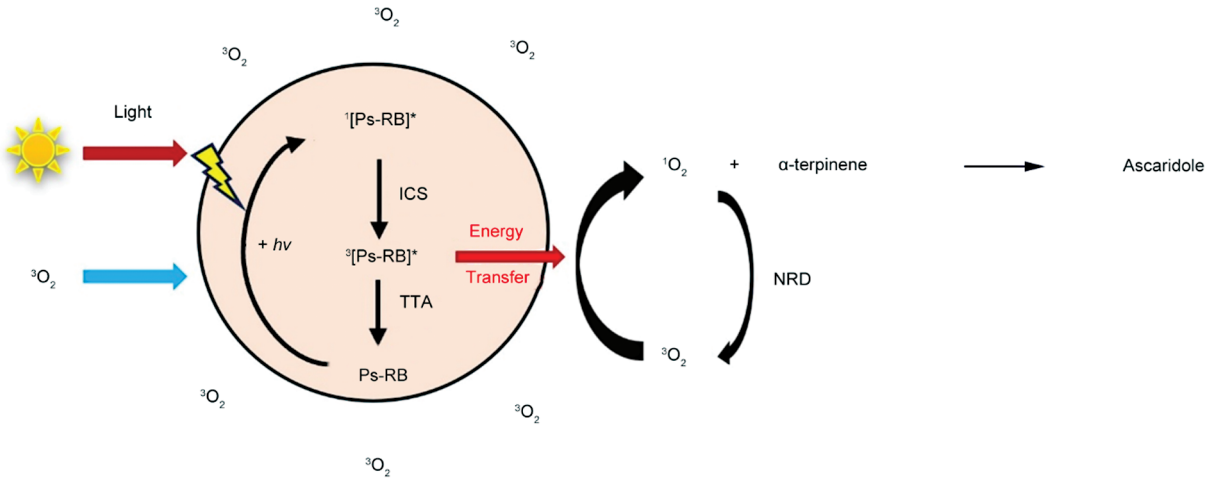

Fig. 1 Reaction scheme of $^1O_2$ photosensitization by Ps-RB and subsequent photooxidation of α-terpinene to produce ascaridole. NRP, non-radiative decay; $^1O_2$, singlet oxygen; Ps-RB, polymer-supported rose Bengal.

step is to convert ^{1}[Ps-RB]* to a triplet excited state (^{3}[Ps-RB]*) via intersystem crossing (ISC), through which energy transfer from ^{3}[Ps-RB]* to ground state triplet molecular oxygen ($^3O_2$) occurs and produces $^1O_2$, at the same time ^{3}[Ps-RB]* returns to its initial ground state (Ps-RB) via triplet–triplet annihilation (TTA). $^1O_2$ readily reacts with α-terpinene in solution to yield ascaridole, in parallel $^1O_2$ spontaneously decomposes to $^3O_2$ via nonradiative decay through vibronic energy transfer with solvent molecules (►**Fig. 1**). $^1O_2$ exists as a gas but is dissolved in the reaction mixture or solvent,[17] chloroform ($CHCl_3$) in this work, as it provides the longest $^1O_2$ lifetime of all common, nondeuterated laboratory solvents.[18]

Heterogeneous photosensitizers are generally composed of organic dyes bearing a (hetero)aromatic core, e.g., rose Bengal (RB). Because RB suffers from extensive photobleaching/degradation under prolonged irradiation, the leaching is usually difficult to be removed from reaction effluents[19,20]; modifications in synthesis have led to various robust solid photosensitizers. In this work, Ps-RB porous beads are the photosensitizers and have high absorption coefficients in the visible spectral region with its optimal light wavelength of 530 nm.[21] The beads are stable after photosensitization.

Materials

All reagents and solvents were used as received without further purification unless otherwise stated. All organic solvents were sourced from Fisher Scientific at SLR grade; α-terpinene was purchased from the Division of Tokyo Chemical Industry (> 90% purity); RB disodium salt from Alfa Aesar; and chloromethyl polystyrene resins (Ps-CH_2Cl, 0.92 mmol/g w.r.t. CH_2Cl loading, 100–200 mesh) from Rapp-Polymere Gmbh.

Ps-RB beads

Ps-RB beads were synthesized and characterized by our colleagues in the chemistry department according to known literature methods, illustrated in ►**Fig. 2**.[22,23] The loading of RB on the polymer support was assessed by hydrolysis and ultraviolet-visible light absorbance (UV-Vis) spectroscopy, according to the procedure. A sample of the crushed Ps-RB material (20 mg) was added to a vial equipped with a magnetic stirrer bar. Tetrabutylammonium hydroxide solution approximately 1 mol/L in MeOH (3 mL) and 1,4-dioxane (10 mL) were added to the vial. The vial was sealed and stirred magnetically for 24 hours at room temperature. The reaction mixture was then filtered through a sintered glass funnel, and the resins were washed with MeOH until no visible color appeared in the filtering solvent.

The filtrate was transferred into a volumetric flask and diluted to 100 mL with MeOH. The final solvent ratio of the solution was 87:10:3 (MeOH/1,4-dioxane/TBAOH solution). The solution was too concentrated for UV-Vis analysis, so a 1 mL portion of this solution was transferred to a 50 mL volumetric flask and diluted with the same MeOH/1,4-dioxane/TBAOH (87:10:3) solution. From the UV-Vis absorption spectrum of the solution, the amount of free RB was determined, using the molar attenuation coefficient ($\varepsilon = 78{,}028 \pm 1{,}291$ L mol^{-1} cm^{-1} at 556 nm) from the literature for RB in the same solvent mixture. The measured maximum absorbance of the solution was recorded as 0.117 a.u., indicating that 7.5×10^{-3} mmol of RB had been liberated from the polymer sample. This equates to a minimum loading of RB on the Ps-RB material of 0.38 ± 0.006 mmol g^{-1}.

Characterization of the Beads

Our colleagues in the chemistry department analyzed the polymer resins using UV-Vis and Fourier-transform infrared spectroscopy (FTIR). Solution-state UV-Vis spectra were recorded on a Shimadzu UV-2550 system with 10 mm quartz cuvettes. Solid-state UV-Vis spectra were registered on a PerkinElmer Lambda 25 system using a Labsphere RSA-PE-20 reflectance spectroscopy integration sphere. FTIR spectra were read on a PerkinElmer Spectrum 100 FTIR Spectrometer.

Reactor Setup

According to the Beer–Lambert–Bouguer Law, it is essential to have a reactor with a high specific surface area (m^2 m^{-3}) to achieve efficient and complete irradiation to reaction media.

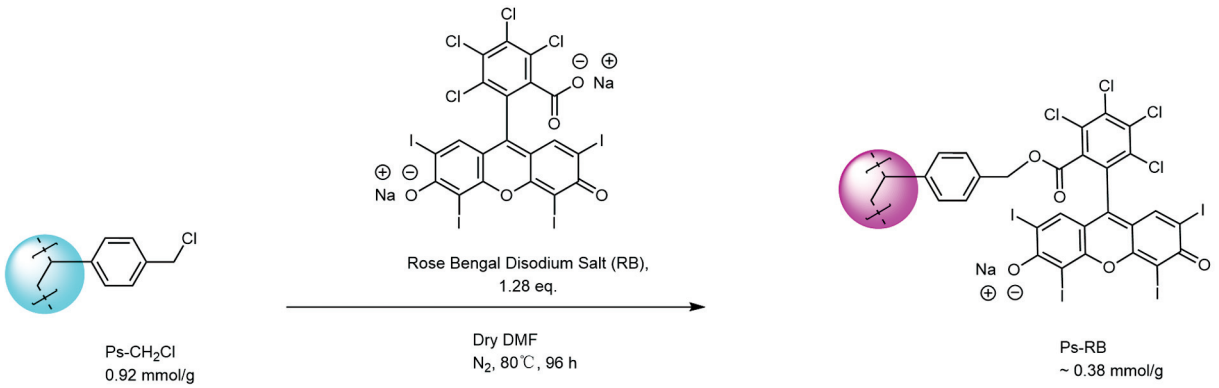

Fig. 2 Reaction scheme for the synthesis of Ps-RB (courtesy of Christopher Thomson).

Due to the high specific surface areas of both the continuous oscillatory baffled reactor and the batch oscillatory baffled reactor, planting light-emitting diodes (LEDs) evenly on the surfaces of orifice baffles enables its length scale to be comparable to the photon penetration depth. The OBPR consists of a glass column of 50 mm in diameter and 480 mm in height as shown in ►**Fig. 3**. The volume of the reactor is 600 mL, with a working volume of 500 mL. Orifice baffles have an outer diameter of 46 mm, a hole diameter of 26 mm, and a baffle spacing of 60 mm. A set comprises three orifice baffles, each baffle has six evenly spaced green LEDs (Cree 5-mm Round LEDs) planted on the lower surface (can also be both sides), as shown in ►**Fig. 3**, to provide light. The wavelength and light intensity of the green LEDs are 530 nm and 0.756 watts, respectively. An air sparger is located at the base of the OBPR for introducing air at a controlled rate.

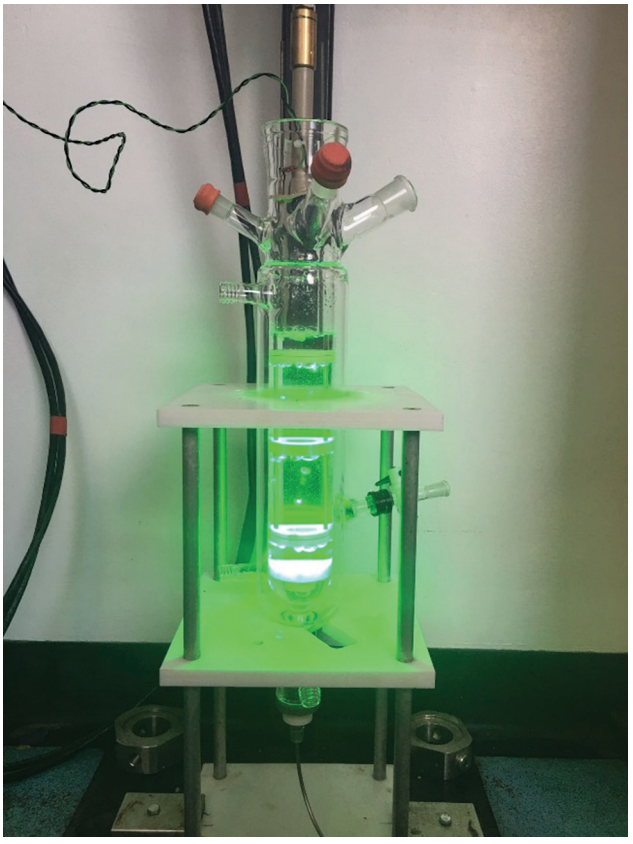

Fig. 3 The schematic of OBPR reactor and orifice baffles with LEDs. OBPR, oscillatory baffled photo reactor.

Analytic Method

Samples were taken regularly from the OBPR and analyzed using proton nuclear magnetic resonance (^{1}H NMR) to determine the composition/concentration of the mixture. The procedure of treating samples was performed as follows:

- Each 2 mL sample containing $CHCl_3$ + α-terpinene + ascaridole was injected into a dark vial to stop the reaction (reaction stops when light is off).
- The sample was placed into a round bottom flask and the solvent ($CHCl_3$) was removed under reduced pressure on a rotary evaporator (40°C, 365 mbar for approximately 5 minutes).
- The oily residue was dissolved in 0.5 mL of deuterated chloroform ($CDCl_3$) and a ^{1}H NMR was obtained (300 MHz Bruker AVIII spectrometer).
- Peaks in the region between 6.70 and 5.40 ppm were used to determine the conversion of α-terpinene and the appearance of ascaridole.

►**Fig. 4** is a typical ^{1}H NMR spectra in chloroform-*d*, showing the alkenyl proton resonances of α-terpinene as a multiplet at 5.61 ppm, and ascaridole as a doublet of doublets centered at 6.45 ppm, which are consistent with previous reports.[24] The resonance signals count for two alkenyl protons of the respective molecules, and as the reaction stoichiometry is in a 1:1 ratio, the integrals of these signals are directly proportional to the relative concentrations of the two species.

Results and Discussion

Based on previous works in a microchannel reactor,[25–27] 390 mL $CHCl_3$ was mixed with 8.47 mL of α-terpinene in the OBPR in the presence of Ps-RB beads. Oscillation frequency and amplitude were switched on once all chemicals were charged into the OBPR, the reaction was initiated when LEDs were turned on, and the duration of the reaction was 120 minutes.

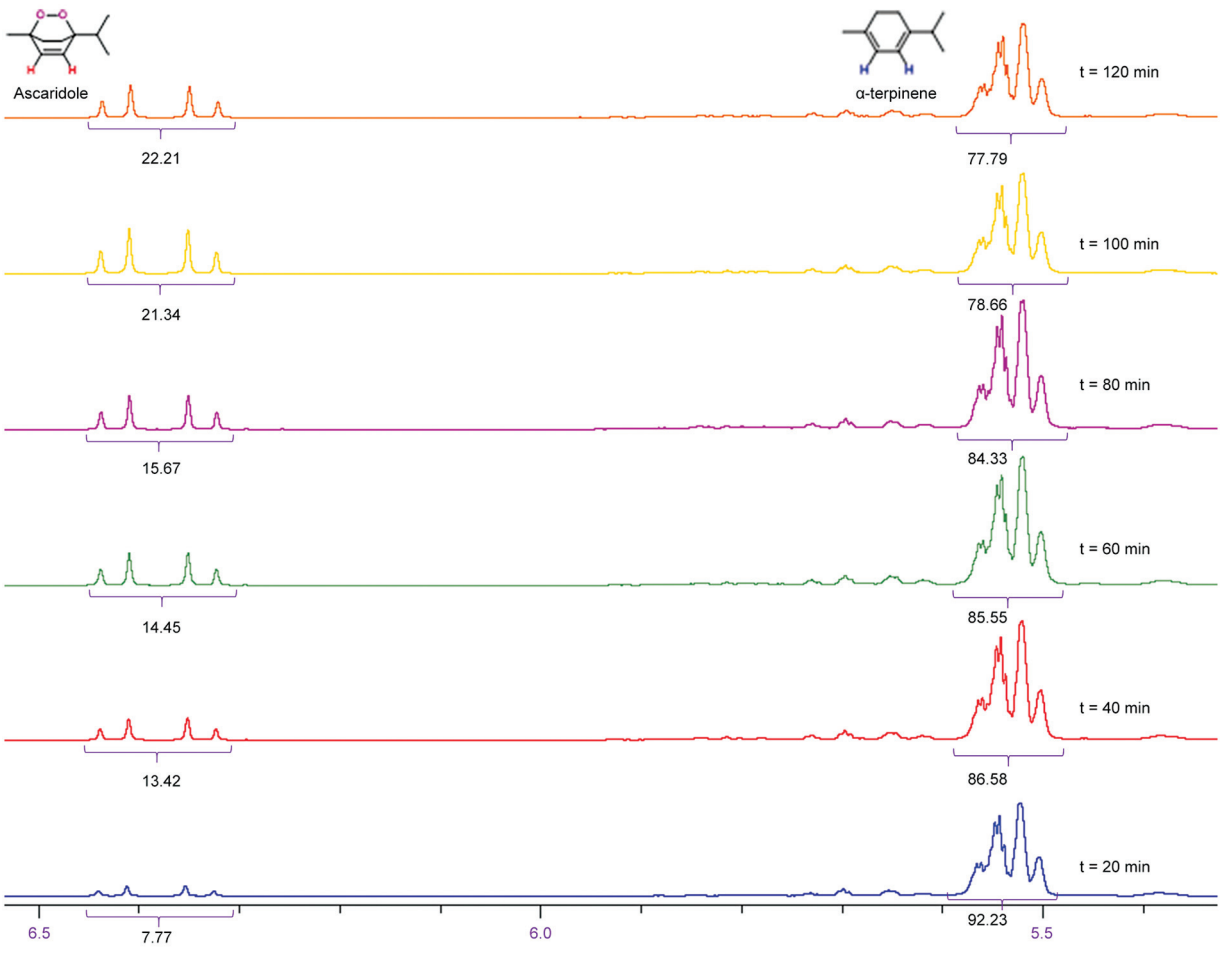

Fig. 4 Stacked ^{1}H NMR spectra for monitoring the conversion of the two alkenyl protons of α-terpinene to ascaridole at an interval of 20 minutes in the OBPR. Photo-oxidation conditions: mass of Ps-RB = 800 mg, irradiation wavelength = 530 nm, oscillation frequency = 2.5 Hz, oscillation amplitude = 24 mm, air flow rate = 172.5 mL min^{-1}. OBPR, oscillatory baffled photo reactor.

Table 1 Experimental conditions (irradiation wavelength = 530 nm, oscillation frequency = 2.5 Hz, oscillation amplitude = 24 mm)

Run number	1	2	3	4	5
Mass of dry beads recovered (mg)	800	690	610	440	370
% Reduction in mass between each run		13.75	11.60	27.87	15.90
Mass of beads used for PSD analysis (mg)	20	20	20	20	20
Mass of beads used for subsequent run (mg)	800	670	590	420	350
Volume of $CHCl_3$ (mL)	390.00	326.63	287.63	204.75	170.63
Volume of α-terpinene (mL)	8.47	7.09	6.25	4.45	3.71
Total liquid volume (mL)	398.47	333.72	293.87	209.20	174.33
Aeration rate (mL min^{-1})	172.5	144	127	91	75
VVM	0.43	0.43	0.43	0.43	0.43
Ratio of α-terpinene/$CHCl_3$	0.022	0.022	0.022	0.022	0.022
Ratio of bead mass/α-terpinene (mg mL^{-1})	94.45	94.50	94.40	94.38	94.34
Ratio of bead mass/liquid volume (mg mL^{-1})	2.008	2.008	2.008	2.008	2.008
D_{10} (μm)	106	116	118	205	187
D_{50} (μm)	148	164	174	1050	1290
D_{90} (μm)	202	229	1660	2350	2450

Abbreviations: PSD, particle size distribution; VVM, volume of air per volume of liquid per minute.

The durability of Ps-RB beads was tested by carrying out the same experiment five times over 5 separate days. Before the first test, the particle size distribution (PSD) and microscopic images of the Ps-RB beads were analyzed in a Malvern sizer and a microscope, respectively. After the end of the first test, the beads were recovered using 10 µm Whatman filter paper, washed using chloroform, and dried overnight. The weight, the PSD, and microscopic images of the used beads were obtained before these were reused in the second run at a reduced liquid volume/composition/air flow rate based on the conditions in Run 1. In doing so, the ratios of α-terpinene over $CHCl_3$, bead mass over α-terpinene, bead mass over the total liquid volume, and VVM (volume of air per volume of liquid per minute) were kept unchanged. This format was repeated in the subsequent runs and the experimental conditions are summarized in ►**Table 1**.

We see from ►**Table 1** that the mass of the beads decreased after each run, due to likely wearing/tearing and fractionation when beads collide with the walls, baffles, and themselves in the OBPR under fluid oscillation. ►**Fig. 5** compiles the microscopic images and the PSD of the beads before each run; the beads were discrete and of spherical in shape in

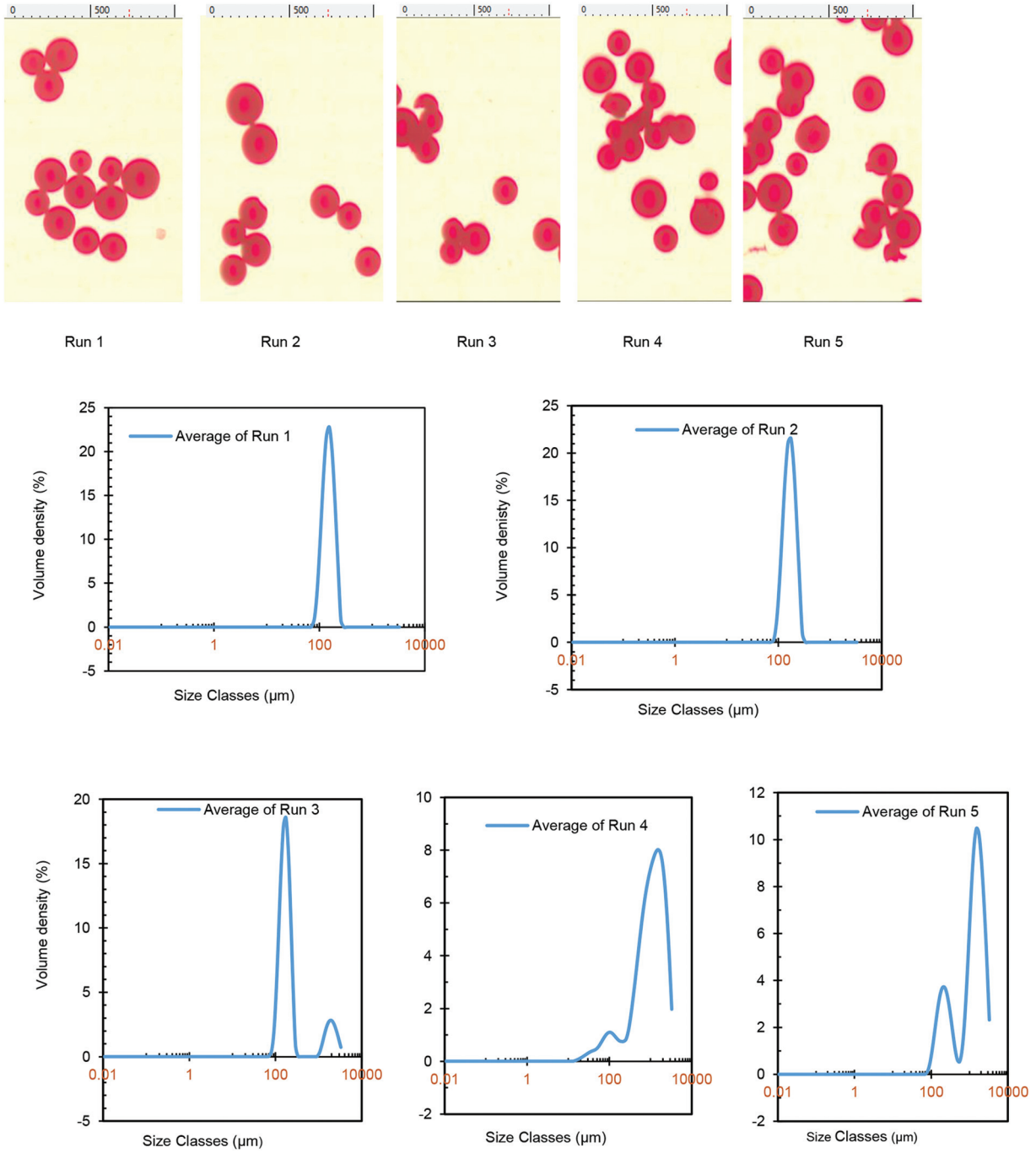

Fig. 5 Microscopic images and PSD of beads for each run. Experimental conditions: irradiation wavelength = 530 nm, oscillation frequency = 2.5 Hz, oscillation amplitude = 24 mm. PSD, particle size distribution.

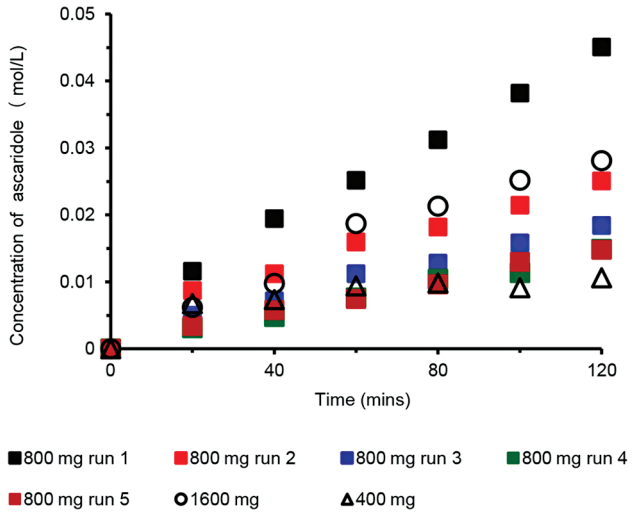

Fig. 6 Durability test of Ps-RB beads after repeated use for conversion of α-terpinene to ascaridole (irradiation wavelength = 530 nm, oscillation frequency = 2.5 Hz, oscillation amplitude = 24 mm).

Run 1 with well-defined PSD, broke up gradually, and agglomerated in the subsequent runs; these are shown as the broader and bimodal PSDs in ►**Fig. 5**, as well as the skewed large particle sizes in D_{90} in ►**Table 1**. The size shifted to the right (becomes bigger) due to the swelling of the beads; the bimodal PSDs are directly related to fractionations of beads and agglomerations of broken pieces with beads.

The results of the durability tests are given in ►**Fig. 6**, demonstrating the gradual and continuous reduction of ascaridole with the increased usage of the Ps-RB. We have validated in our previous work[28] that singlet oxygen is in excess in the given experimental conditions, where the second-order reaction of $^1O_2 + \alpha$-terpinene $\xrightarrow{k3}$ ascaridole is then reduced to a pseudo-first-order reaction of α-terpinene $\xrightarrow{k3}$ ascaridole. By plotting $\ln(C_{\alpha T0}/C_{\alpha T})$ versus time for each run, approximate straight lines can be seen in ►**Fig. 7**, confirming the pseudo-first-order kinetics, where $C_{\alpha T}$ and $C_{\alpha T0}$ are the concentrations of α-terpinene at time t and time $t = 0$ (mol L^{-1}), respectively.

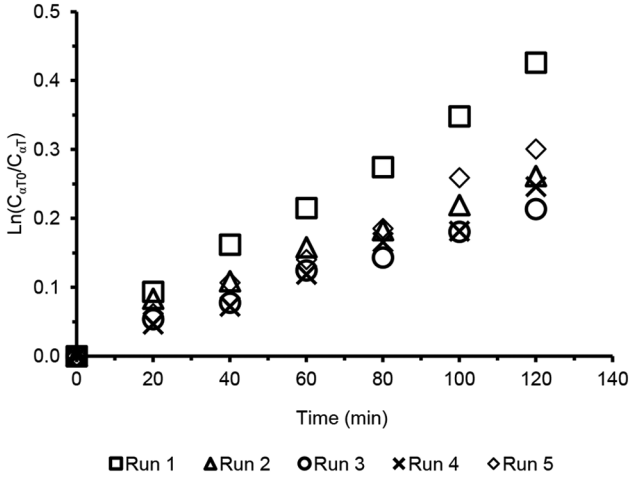

Fig. 7 The pseudo-first-order kinetics fit.

Table 2 First order rate constants for each run

Run number	k (min^{-1})	Dry bead mass (mg)	Durability (%)
1	0.0035	800	100
2	0.0023	690	56.68
3	0.0018	610	39.21
4	0.0020	440	31.43
5	0.0025	370	33.04

The rate constants are the slopes and are summarized in ►**Table 2**.

To assess the durability of the beads, we must consider two aspects: (1) the loss of beads after each run, which leads to the reduction of active specific surface area ($m^2\ m^{-3}$); (2) the reduced product (ascaridole) concentration as shown in ►**Fig. 6**, which is related to the reduced rate constant. The durability of beads (photosensitizer) can thus be defined as Equation (1).

$$\left(\frac{Mass\ of\ beads_{run(n+1)}}{Mass\ of\ beads_{run1}} \times \frac{k_{run(n+1)}}{k_{run1}}\right) \times 100\%$$

$$n = 1\ to\ 4 \qquad (1)$$

When there is no loss of beads, the specific surface area would be the same for Run 1 and Run 2 for instance, so would be the rate constant, and the durability would then be 100%. The durability for each run is included in ►**Table 2**; we see that the durability of the beads has reduced by 2/3 after five consecutive runs.

Taking the analogy to the half-life of the catalyst, the half-life of the beads' durability can then be defined as the amount of time needed for the maximum concentration of α-terpinene (0.13 mol/L) to decrease by half, which for a pseudo-first-order reaction is expressed as $t_{1/2} = \ln 2/k_{run1} = 198$ minutes.

The effect of the mass of Ps-RB beads on the consumption of α-terpinene and the generation of ascaridole was also investigated using three mass loadings of 400, 800, and 1,600 mg, respectively, as shown in ►**Fig. 6** at fixed oscillation conditions, light wavelength, and intensity. We see that the ascaridole concentration was very low at a loading of 400 mg of the beads, indicating insufficient surface areas for photo absorption. On the other hand, there were too many beads in the OBPR at 1,600 mg and the overlaps of beads blocked the light penetration, leading to reduced activities for photo absorption. It seems that the loading of 800 mg of beads was the optimal amount for the OBPR, leading to enhanced exchanging energy available via the Type II reaction mechanism.[29] When photons of the correct wavelength (<600 nm) irradiate the photosensitizer material (Ps-RB), the supported RB chromophore is electronically excited and converts to a triplet state via ISC, which enables it to undergo an energy transfer, a TTA process with oxygen to produce singlet oxygen.[30,31] The lifetime of singlet oxygen depends on temperature and solvent environment as vibronic energy transfer with solvent is a competitive, nonproductive process

which returns $^1O_2$ to its ground state, $^3O_2$.[32] Due to the energy barrier (94 kJ/mol), $^3O_2$ molecules cannot directly be excited to $^1O_2$ due to it being a forbidden electronic transition by spin selection rules and therefore requires a triplet photosensitizer to enable the TTA energy transfer mechanism.[33] As a result, the optimal amount of photosensitizer presents a higher concentration of triplet excited states that can produce $^1O_2$.[34] In this work, 800 mg was identified as the optimal mass of beads in the OBPR under the experimental conditions investigated.

Conclusion

In this article, we have presented, for the first time, the results of the durability tests of Ps-RB beads in the reaction between α-terpinene and singlet oxygen. By recovering and reusing the beads in appropriate ratios in subsequent runs, we discovered that the mass of the beads decreased, the beads broke down and agglomerated as the usage of the beads increased. Based on the pseudo-first-order kinetics, the rate constants were evaluated for each run. We have then proposed a methodology for assessing the durability of the beads taking into consideration both the loss of bead mass and the reduced rate constant. Our data indicate that the durability was reduced by two-thirds after five consecutive runs, the half-life of the durability was estimated and can be reached at less than 200 minutes. Finally, we have also identified the optimal mass of the beads in the OBPR.

Note

$C_{\alpha\text{-}T}$: concentration of α-Terpinene at time = t (mol L^{-1}).
$C_{\alpha\text{-}T0}$: concentration of α-Terpinene at time = 0 (mol L^{-1}).
f: oscillation frequency (Hz).
x_o: oscillatory center-to-peak amplitude (m).

Conflict of Interest

None declared.

Acknowledgments

The authors wish to express special thanks to Christopher Thomson and Dr. Filipe Vilela, Institute of Chemistry Science, Heriot-Watt University for supplying photosensitizers, and the associated information for synthesis and characterization. The authors also wish to thank Andrew Haston for fabricating the LED baffles and Douglas Wagener for constructing the experimental rigs.

References

1 Abdiaj I, Alcázar J. Improving the throughput of batch photochemical reactions using flow: dual photoredox and nickel catalysis in flow for C(sp^2)C(sp^3) cross-coupling. Bioorg Med Chem 2017;25(23):6190–6196
2 McCarver SJ, Qiao JX, Carpenter J, et al. Decarboxylative peptide macrocyclization through photoredox catalysis. Angew Chem Int Ed Engl 2017;56(03):728–732
3 Kölmel DK, Loach RP, Knauber T, Flanagan ME. Employing photoredox catalysis for DNA-encoded chemistry: decarboxylative alkylation of α-amino acids. ChemMedChem 2018;13(20):2159–2165
4 Konev MO, McTeague TA, Johannes JW. Nickel-catalyzed photoredox-mediated cross-coupling of aryl electrophiles and aryl azides. ACS Catal 2018;8:9120–9124
5 Oderinde MS, Jones NH, Juneau A, et al. Highly chemoselective iridium photoredox and nickel catalysis for the cross-coupling of primary aryl amines with aryl halides. Angew Chem Int Ed Engl 2016;55(42):13219–13223
6 Knauber T, Chandrasekaran R, Tucker JW, et al. Ru/Ni dual catalytic desulfinative photoredox $C_{sp}{}^2$-$C_{sp}{}^3$ cross-coupling of alkyl sulfinate salts and aryl halides. Org Lett 2017;19(24):6566–6569
7 Bottecchia C, Lévesque F, McMullen JP, et al. Manufacturing process development for belzutifan, part 2: a continuous flow visible-light-induced benzylic bromination. Org Process Res Dev 2022;26:516–524
8 Sing S, Roy WJ, Dagar N, Sen PP, Roy SR. Photocatalysis in dual catalysis systems for carbon-nitrogen bond formation. Adv Synth Catal 2020;363:937–979
9 Corcoran EB, McMullen JP, Lévesque F, Wismer MK, Naber JR. Photon equivalents as a parameter for scaling photoredox reactions in flow: translation of photocatalytic C-N cross-coupling from lab scale to multikilogram scale. Angew Chem Int Ed Engl 2020;59(29):11964–11968
10 Robinson A, Dieckmann M, Krieger JP, et al. Development and scale-up of a novel photochemical C–N oxidative coupling. Org Process Res Dev 2021;25:2205–2220
11 Lévesque F, Di Maso MJ, Narsimhan K, Wismer MK, Naber JR. Design of a kilogram scale, plug flow photoreactor enabled by high power LEDs. Org Process Res Dev 2020;24:2935–2940
12 Lapierre R, Thi Le TM, Schiavi B, et al. Photocatalytic and photoinduced phosphonylation of aryl iodides: a batch and flow study. Org Process Res Dev 2023
13 Ren H, Maloney KM, Basu K, et al. Development of a green and sustainable manufacturing process for gefapixant citrate (MK-7264) part 1: introduction and process overview. Org Process Res Dev 2020;24:2445–2452
14 Baumann M, Baxendale IR. Continuous photochemistry: the flow synthesis of ibuprofen via a photo-Favorskii rearrangement. React Chem Eng 2016;1:147–150
15 Li Q. Liu M, Jiang M, Wan L, Ning Y, Chen FE. Photo-induced 1,2-aryl migration of 2-chloro-1-arylpropanone under batch and flow conditions: Rapid, scalable and sustainable approach to 2-arylpropionic acids. Chin Chem Lett 2023
16 Plutschack MB, Pieber B, Gilmore K, Seeberger PH. The Hitchhiker's guide to flow chemistry ||. Chem Rev 2017;117(18):11796–11893
17 Villén L, Manjón F, García-Fresnadillo D, Orellana G. Solar water disinfection by photocatalytic singlet oxygen production in heterogeneous medium. Appl Catal B 2006;69:1–9
18 Ogilby PR, Foote CS. Chemistry of singlet oxygen. 42. Effect of solvent, solvent isotopic substitution, and temperature on the lifetime of singlet molecular oxygen (1.DELTA.g). J Am Chem Soc 1983;105:3423–3430
19 Whitmire C. Photosensitizers: Types, Uses and Selected Research. eds. New York, NY: Nova Science Publishers; 2016
20 Gianotti E, Martins Estevão B, Cucinotta F, et al. An efficient rose bengal based nanoplatform for photodynamic therapy. Chemistry 2014;20(35):10921–10925
21 Deshpande MS, Rale VB, Lynch JM. Aureobasidium pullulans in applied microbiology: a status report. Enzyme Microb Technol 1992;14:514–527
22 Burguete MI, Galindo F, Gavara R, et al. Singlet oxygen generation using a porous monolithic polymer supported photosensitizer: potential application to the photodynamic destruction of melanoma cells. Photochem Photobiol Sci 2009;8(01):37–44
23 Fabregat V, Burguete MI, Galindo F, Luis SV. Singlet oxygen generation by photoactive polymeric microparticles with

enhanced aqueous compatibility. Environ Sci Pollut Res Int 2014; 21(20):11884–11892
24 Zhang K, Kopetzki D, Seeberger PH, Antonietti M, Vilela F. Surface area control and photocatalytic activity of conjugated microporous poly(benzothiadiazole) networks. Angew Chem Int Ed Engl 2013;52(05):1432–1436
25 Dong Z, Wen Z, Zhao F, Kuhn S, Noël T. Scale-up of micro- and milli-reactors: an overview of strategies, design principles and applications. Chem Eng Sci: X 2021;10:100097
26 Kuijpers KPL, van Dijk MAH, Rumeur QG, Hessel V, Su Y, Noël T. A sensitivity analysis of a numbered-up photomicroreactor system. React Chem Eng 2017;2:109–115
27 Thomas CG, Jones CMS, Rosair G, et al. Continuous-flow synthesis and application of polymer-supported BODIPY Photosensitisers for the generation of singlet oxygen; process optimised by in-line NMR spectroscopy. J Flow Chem 2020;10:327–345
28 Chen JH, Prinsloo R, Ni X. A kinetic study of a photo-oxidation reaction between α-terpinene and singlet oxygen in a novel oscillatory baffled photo reactor. ChemPhotoChem 2023
29 Baptista MS, Cadet J, Di Mascio P, et al. Type I and type II photosensitized oxidation reactions: guidelines and mechanistic pathways. Photochem Photobiol 2017;93(04):912–919
30 Hockey RM, Nouri JM. Turbulent flow in a baffled vessel stirred by a 60° pitched blade impeller. Chem Eng Sci 1996;51:4405–4421
31 Tobin JM, McCabe TJD, Prentice AW, et al. Polymer-supported photosensitizers for oxidative organic transformations in flow and under visible light irradiation. ACS Catal 2017;7:4602–4612
32 Zhao J, Wu W, Sun J, Guo S. Triplet photosensitizers: from molecular design to applications. Chem Soc Rev 2013;42(12): 5323–5351
33 Erickson PR, Moor KJ, Werner JJ, Latch DE, Arnold WA, McNeill K. Singlet oxygen phosphorescence as a probe for triplet-state dissolved organic matter reactivity. Environ Sci Technol 2018;52 (16):9170–9178
34 Wilkinson F, Helman WP, Ross AB. Rate constants for the decay and reactions of the lowest electronically excited singlet state of molecular oxygen in solution. an expanded and revised compilation. J Phys Chem Ref Data 1995;24:663–677